# Effects of the heating source on the regeneration performance of different adsorbents under post-combustion carbon capture cyclic operations. A comparative analysis

M.M. Yassin[a], J.A. Anderson[a], G.A. Dimitrakis[c], C.F. Martín[a,b],* cfmartin@abdn.ac.uk

[a]University of Aberdeen, School of Engineering, Materials and Chemical Engineering Group, Fraser Noble Building, King's College, Aberdeen AB24 3UE, Scotland, United Kingdom

[b]Centre for Energy Transition, University of Aberdeen, United Kingdom

[c]Department of Chemical and Environmental Engineering, Faculty of Engineering, University of Nottingham, University Park, Nottingham NG7 2RD, United Kingdom

*Corresponding author at: University of Aberdeen, School of Engineering, Materials and Chemical Engineering Group, Fraser Noble Building, King's College, Aberdeen AB24 3UE, Scotland, United Kingdom.

## Abstract

This work presents a comparative study of microwave and conventional (conductive) heating for adsorbent regeneration. A binary gas mixture representative of pre-dried flue gas from coal-fired power plants (15% v/v $CO_2$ in $N_2$) was passed through a rotary fixed-bed adsorption column filled with a zeolite molecular sieve (13X) and an activated carbon (Norit R2030CO$_2$). The impact of the two regeneration methods on both the textural properties and the carbon capture performance ($CO_2$ uptake capacity, regeneration efficiency, and rate of regeneration) were assessed and compared after consecutive adsorption/desorption cycles. Overall, Norit R2030CO$_2$ maintained stable adsorption capacity and regeneration efficiency with both conventional and microwave heating but slightly better with the latter. Additionally, power consumption per adsorbent unit mass and per adsorbate removed were reduced with microwave regeneration by 18.69 and 17.76% respectively compared to conventional regeneration. In the case of 13X, adsorption capacity and regeneration efficiency were found to be relatively stable after a drop in the first cycle in both heating modes, whereas power requirement was found higher in microwave regeneration than in conventional regeneration.NoritR2030CO$_2$ showed a slightly higher maximum desorption rate when regenerated with microwave heating compared to conductive heating. Contrarily, the maximum desorption rate for the molecular sieve is higher with conductive heating as opposed to microwave heating. However, the data indicated a bigger desorption rate with the microwave regeneration in both adsorbents in later stages of the heating process (i.e. from min 16th for NoritR2030CO$_2$ and from min 18th for 13X until process completion). The breakthrough time ($t_b$) of Norit R2030CO$_2$ was unaffected by cyclic operation or the heating methods, whereas in 13X this value varied over the cycles. The latter observation indicates that 13X requires either longer times or higher temperatures to achieve full regeneration compared to Norit R2030CO$_2$.It can be concluded that microwave-assisted regeneration presented slight advantages over regeneration with conductive heating in delivering more steady capture capacity and regeneration efficiency for Norit R2030CO$_2$ under the test conditions employed here whereas 13X exhibited indifference.

## 1 Introduction

Despite the growing consensus of carbon capture, storage (CCS), and carbon capture, storage, and utilisation (CCUS) being a necessity in the global fight against $CO_2$ emissions, its full-scale implementation is yet to be achieved. The

main challenge in power plants is the high energy penalty associated with the capture process involved in any CCS/CCUS process. The currently most developed and deployed amine scrubbing process has characteristic barriers to implementation such as intensive solvent regeneration energy, high solvent losses and degradation, and equipment corrosion [1]. A very promising and viable alternative to overcome those technical drawbacks is adsorption using porous solid materials with high capture capacity and selectivity towards $CO_2$ [2–4]. However, it also presents some challenges, such as high feed gas loss in the bed after venting out during the de-pressuring step, and the energy consumption associated with the pressurisation in pressure awing Adsorption (PSA) processes [5]. Long cycle times, high energy consumption during regeneration, and heat transfer limitations are some of the most relevant drawbacks identified for thermal swing adsorption (TSA) processes due to extended heating and cooling periods [6,7]. As an alternative to TSA, microwave swing adsorption (MWSA) has been proposed by some researchers as a potentially more efficient heating source, hence a novel regeneration alternative. Microwave heating of sorbents has been advocated for several advantages over conventional heating, the main being that adsorbents can selectively and directly be heated avoiding the energy consumed in transferring the heat across the adsorption column. Accordingly, volumetric microwave heating could make the gas separation process more energetically efficient. In this work we compared the energy requirements for the regeneration to take place using both, an adapted conductive heating source at laboratory scale, and a multimode microwave cavity. Both pieces of equipment were connected to the mains to get the power required for the regeneration, however it is worth to mention that in a practical term, in TSA process at industrial scale the whole energy needed to run the thermal swing may not necessarily come from the mains, as waste heat integration is likely to provide a portion or the whole energy needed. In this work, to be able to compare both heating technologies to perform the thermal swing, we have considered energy requirement assuming both options are fed by the electric mains.

Cherbanski et al. studied MWSA and TSA of acetone and toluene from 13X molecular sieves and concluded that microwave heating provided a faster heating rate, lower power consumption, and therefore shorter cycle time and less energy expenditure than conventional heating [8]. Di and Chang investigated microwave regeneration of volatile organic compounds (VOCs) and suggested that microwave heating enhances the desorption rate through a pressure driven mass transfer from adsorbed state to a gaseous state [9]. An activated carbon loaded with n-dodecane was regenerated with both microwave and conductive heating by Fayez et al. They reported that the microwave energy needed to completely regenerate the adsorbents was 6% of that required with conductive heating because of the higher heating rates and reduced heat loss obtained with the former. From a post-regeneration analysis of the activated carbon, no effect on their physical and chemical properties by either of the methods was revealed [10].

Cherbanski has recently compared microwave and conductive heating regeneration of granulated activated carbon saturated with toluene. He concluded that the desorbed mass profiles of toluene practically overlap when the same active power is used irrespective of the regeneration method [11]. This is contrary to previous findings reported which claim that microwave heating guarantees superior regeneration rate and efficiency with activated carbons [10,12]. A study conducted by Çalışkan et al. found that when the nature of the adsorbate is considered, microwave heating does not always guarantee a better performance of activated carbons upon cycling. In their study, an activated carbon was saturated with a pharmaceutical (promethazine) and regenerated with microwave heating and conductive heating. When a mild regeneration temperature was used a fall in adsorption capacity was obtained due to thermal cracking of the adsorbate molecules in the pores. They found this effect more pronounced with microwave regeneration. A phenomenon they called 'microwave-lysis' occurred where direct interaction between the microwave radiation and the adsorbate led to pore blockage due to decomposition of the promethazine inside the pores [13].

Activated carbons (ACs) loaded with $SO_2$ from flue gas were regenerated with microwaves by Zhang et al. The group reported the adsorptive capacity of the microwave regenerated ACs for $SO_2$ exceeded that of the virgin AC, when microwave power used was in the range of 200 to 400 W. They found that surface area, pore volume and the surface acidic functional groups were increased after microwave heating [14]. Emine et al. performed microwave-assisted regeneration of phenol and p-nitrophenol on commercial activated carbons. Despite a slight decrease in surface area and pore volume after heating, it was observed that the adsorbents maintained their adsorption capacity over multiple adsorption-desorption cycles [15].

Vacuum swing regeneration (VSR) assisted with microwaves was studied by Webley and Zhang using wet and dry flue gas (12% v/v $CO_2$ in $N_2$) and zeolite 13X. It was found that $CO_2$ purity in the outlet stream was enhanced by 20% due to the addition of MW heating in the process. When the flue gas was wet, water was responsible for absorbing MW radiation, then the temperature increase was lower than expected because the desorption of water (a strong microwave absorber) attenuated the temperature rise in the bed [16].

Granular activated carbons regenerated with microwave and conventional heating were compared by Chronopoulos et al. for their $CO_2$ desorption rate. Results showed that the overall desorption rate was four times faster for microwave heating in comparison to conventional heating at a similar regeneration temperature [17]. $CO_2$ adsorption capacity, desorption rate, stability after cycles, and dielectric heating of amine functionalised mesoporous silica (MCM-48) was recently tested by Nigar et al. They found that as the amino groups on the surface were increased, both the $CO_2$ adsorption capacity and susceptibility to microwave absorption are increased. Four times faster desorption rate was

achieved under microwave heating compared to conventional heating. The material was therefore considered suitable for microwave-swing regeneration as the capture capacity was preserved over 20 cycles [18]. Yang et al. performed a microwave-assisted regeneration of spent per-fluorinated silica-stabilized dry alkanolamines ($DA_f$) previously saturated with $CO_2$. $DA_f$ displayed excellent stability in swing absorption - regeneration cycles [19].

This study investigates the potential of direct microwave heating to reduce the energy requirement involved in the adsorbent regeneration process for post-combustion capture in coal fired power plants. Accordingly, microwave-assisted swing regeneration and temperature swing regeneration were investigated using two widely used adsorbents and a simulated pre-dried flue gas mixture. In this work, a detailed and comprehensive comparative study was conducted on multi-cyclic MWSA and TSA experiments. Comparison of the two regeneration methods was mainly based on key process parameters such as regeneration efficiency, regeneration rate, and sorbent stability after adsorption-regeneration cycles. To the best of our knowledge, this is the first time that a comprehensive comparative work between microwave regeneration and thermal conductive regeneration has been carried out on these adsorbents and with the process conditions applied here for a post-combustion carbon capture process. The detailed manner in which the adsorption- and regeneration-related process parameters are evaluated provides additional insight compared to previously reported results.

## 2 Materials and methods

### 2.1 Materials and adsorbent characterisation

#### 2.1.1 Materials

Commercial adsorbents Norit R2030CO$_2$ (from now, Norit R) and zeolite 13X (from now, 13X) were donated from Cabot and purchased from Alfa Aesar, respectively. Norit R is an extruded, steam activated peat-based carbon with 2–3 mm particle diameter, and it is specifically designed for $CO_2$ removal. Zeolite 13X is a pellet-form molecular sieve with 1–2 mm particle diameter. 13X is a faujasite type zeolite (Si/Al ~1.0–1.4) with high sodium cation density in its framework [20]. Ultrahigh purity gases (99.995–99.998%) were used for all measurements and were provided by BOC UK.

#### 2.1.2 Adsorbent characterisation

The samples were characterised by $N_2$ adsorption/desorption isotherms at −196 °C. The $N_2$ isotherms were measured in a Micromeritics Tristar 3000 V5.00 apparatus. Prior to any measurement, the samples were outgassed with $N_2$ at 300 °C with a heating rate of 3 °C/min for approximately 12 h. The BET surface area ($S_{BET}$), total pore volume ($V_p$) and pore size distribution (PSD) were determined from the $N_2$ isotherms at −196 °C. The surface area was calculated using the Brunauer-Emmett-Teller (BET) equation, and the total pore volume ($V_p$) was calculated from the adsorbed nitrogen after complete pore condensation at $p/p_0 = 0.9905$ by applying Gurvich's rule [21]. PSD was calculated using density functional theory (DFT)- slit pore and NLDFT equilibrium model. A fully detailed textural and chemical characterisation of Norit R was reported previously [22], however, it was also measured here to provide a baseline against which any changes induced by submission to cyclic microwave heating could be determined.
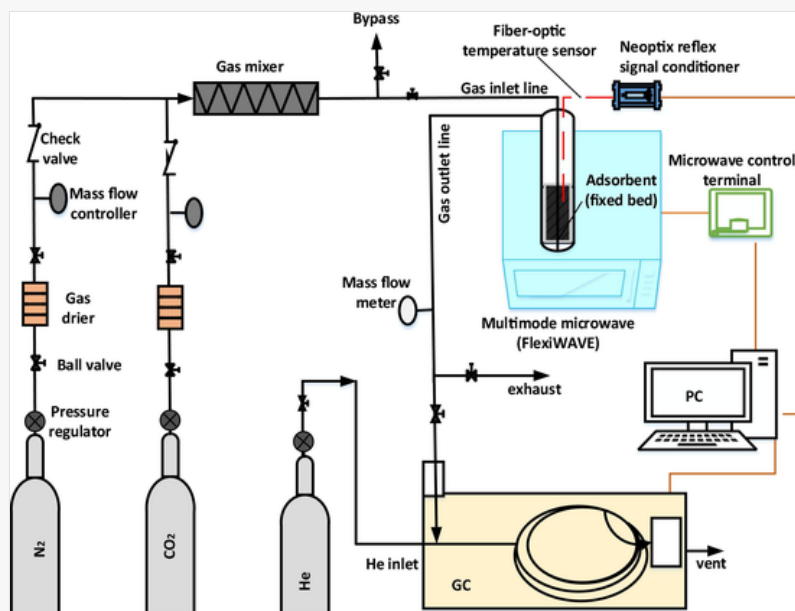
Chemical characterisation was performed by ultimate analysis and $pH_{PZC}$ (Point of Zero Charge). A mass titration method adapted from Noh and Schwarz was used for this purpose [23]. The latter was measured to obtain information about the acid or basic character of the adsorbents employed. Chemical characterisation is included in SI.

Dielectric properties of 13X and Norit R were measured applying the resonant cavity perturbation technique at the University of Nottingham. The applied instrument comprised a cylindrical copper cavity connected to an HP 8753B vector network analyser (VNA), incorporated with a digitally controlled furnace. The sample was placed in a quartz tube and measurements were made at 2450 MHz for all runs. The measured parameters were frequency shift and quality factor from which complex permittivity was evaluated using perturbation theory. The dielectric constant ($\varepsilon'$) and loss factor ($\varepsilon''$) were measured while heating samples from 20 to 500 °C at 5 °C/min heating rate.

### 2.2 Experimental apparatus and procedure:

#### 2.2.1 Experimental apparatus

Fig. 1 shows the schematic diagram of the experimental apparatus used for this study. It consists of a multimode microwave cavity which operates at 2.45 GHz (FlexiWAVE from Milestone, Italy), two EL-FLOW digital mass flow controllers (MFCs) and a EL-FLOW digital mass flow meter (Bronkhorst), a fibre optic sensor connected to a multichannel reflex signal conditioner (from Elliot scientific), a single channel 490-PRO Micro Gas Chromatograph (micro-GC) from Agilent Technologies, fitted with a thermal conductivity detector (TCD) in which He is used as the carrier gas, and a PC for data acquisition and instrument control. In each experiment, the gas composition and flow rate were adjusted using the upstream MFCs, and the outlet total flow rate was measured downstream by the mass flow meter (MFM). The concentration of the off-gas stream components was monitored and recorded online by the micro-GC.

The gas manifold system consists of two lines both fitted with a stainless-steel gas dryer column filled with an equal amount of two desiccants (i.e. zeolite 13X and orange beaded self-indicating silica gel). After passing through the dryers the flow rate of each gas feeding line was controlled with a MFC. The MFCs have an accuracy of 1% full scale and a repeatability of 0.2% RD (percentage of reading). One of the lines is used to feed the inert ($N_2$) to clean and dry the sample before each experiment, and to prepare the binary mixture. The other line is used to feed in $CO_2$. The two lines are joined downstream of the MFCs after which a coiled pipe is located to ensure complete mixing before the feed gas enters the reactor. Therefore, a gas mixture akin to the composition representative of pre-cleaned flue gas from coal-fired power plants can be prepared (i.e. 15% v/v $CO_2$ in $N_2$). A bypass located after the gas mixer and prior to the reactor inlet was fitted to allow flexibility during experiment preparation.

The borosilicate glass reactor is 180 mm in height and 22 mm in internal diameter and is equipped with a porous frit (0 porosity grade) located 11 mm from the base of the reactor. A fibre optic sensor was located at the centre of the reactor at 10 mm above the porous plate. The latter continuously monitored the adsorbent temperature with an accuracy of $\pm 1$ °C. An infrared (IR) temperature sensor embedded in the microwave cavity wall was calibrated against the fibre optic probe and used to provide feedback to the magnetron, so the adsorbent temperature was monitored and controlled by a loop system. The latter was performed to measure the temperature of the adsorbent for MWSA and overcome the limited transmission of the IR sensor through the borosilicate glass reactor. Downstream of the reactor and outside the microwave cavity, gases were continuously analysed with a micro-GC fitted with Hayesep A 40 cm heated single channel column and a TCD. The TCD response was routinely calibrated by employing $CO_2/N_2$ mixtures of known composition.

### 2.2.2 Dynamic TSA and MWSA cycles

Maximum $CO_2$ adsorption capacity under dynamic conditions was measured from the breakthrough curves for the selected adsorbents. Experiments were performed in the fixed/rotary adsorption unit (Fig. 1) using a gas mixture composed of 15% v/v $CO_2$ in $N_2$ representative of pre-cleaned and dry flue gas. The adsorption process was terminated when the TCD signals remained constant overtime, (30 $\pm$ 3 min standard deviation for Norit R and 65 $\pm$ 4 min standard deviation for 13X) indicating full saturation of the bed. The rotation speed of the reactor was adjusted to ensure temperature uniformity within the bed during the MWSA (Microwave Swing Adsorption) experiments.

In a typical experiment, the bed was packed with 6 g of adsorbent. In a representative cyclic adsorption–desorption experiment, prior to adsorption, the adsorbents were degassed at 300 °C overnight with 20 NmL/min $N_2$ gas flow in an electric furnace equipped with a PID controller. The outgassed sample was weighted on a Fisher-brand balance (FAS64, readability 0.0001 g) and loaded into the reactor, after which a pre-conditioning step (samples were purged with 150 ml/min of $N_2$ for 40 min) was followed. The adsorption step was followed by switching the feed to 100 NmL/min of the binary gas mixture (15% v/v $CO_2$ in $N_2$) at room temperature (approximately 23 °C) and 1 bar. The $CO_2$ composition in the effluent gas was continuously monitored as a function of time until the composition approached the inlet gas composition, i.e., until saturation was reached (breakthrough curve). After saturation, the $CO_2$ was desorbed by switching to a 20 NmL/min of $N_2$ feed and raising the temperature to 100 °C (+/-3 °C) for 45 mins

for Norit R, and 65 mins for 13X, in both regeneration methods (MWSA & TSA). Adsorbents were subjected to 12 consecutive adsorption–desorption cycles and their maximum $CO_2$ adsorption capacity was assessed in each cycle.

For MWSA experiments, a 60 mL reactor holding the same quantity of sample (6 g) which occupies 13 cm$^3$ for Norit R and 8 cm$^3$ for 13X was mounted inside the microwave cavity. A continuous variable power output operating at 2.45 GHz frequency was applied to maintain and control the pre-set temperature of the adsorbent during regeneration. TSA experiments were conducted using the same set up, therefore using the same reactor. In this case, microwave heating was substituted for a conductive heating source provided by an electric tape heater (FGR-030-Omega) connected to a 240 V output (max) variable autotransformer (Variac). Adsorbent final temperature and heating ramp were controlled by manually adjusting the voltage output of the Variac during regeneration. The adsorbent temperature during regeneration was monitored with a K-type thermocouple (RS pro) located 10 mm above the porous plate, and 11 mm from the internal reactor wall. The thermocouple was connected to the 2-channel digital thermocouple interface (RS Pro 55II Dual Channel K & J-Type) for online data acquisition. Heating was terminated when the TCD no longer detected $CO_2$ eluted from the reactor outlet. Fig. 2 shows the graphic representation of the different areas considered for the calculation of $CO_2$ adsorbed and desorbed in the experiments. For the latter, the $CO_2$ concentration was plotted versus the time for the adsorption and regeneration steps. The areas under and above the curves, estimated using the trapezoidal rule of numerical integration for definite integral, were used to calculate the amount of $CO_2$ adsorbed (AAC) and regenerated (AUC), using the following equations:

$$AAC = (A_1 + B) = (t_1 - t_0)\, 0.15 + \sum (C_i - C_{i-1}) \left( \frac{t_i + t_{i-1}}{2} \right) \tag{1}$$

$$AUC = ((A_2)) = \sum (t_i - t_{i-1}) \left( \frac{c_i + c_{i-1}}{2} \right) \tag{2}$$

$$q_{ret} = Q\rho(A_1 + B) \tag{3}$$

$$q_{rem} = Q\rho(A_2) \tag{4}$$

where, $Q$ is the inlet total volumetric flow rate (mL/min), $\rho$ is the $CO_2$ density at STP (mg/cm$^3$), $q_{ret}$ is the amount of $CO_2$ retained in the bed (mg), $q_{rem}$ is the amount of $CO_2$ removed from the bed (mg), $t$ is the total process time (min) and $C$ is $CO_2$ concentration (% v/v). $t_0$ is the starting time of the process, $t_1$ is the time just before $CO_2$ is detected at the outlet by the GC. $C_i$ and $C_{i-1}$ are the concentrations of the gas recorded at $t_i$ and $t_{i-1}$ respectively.



Fig. 2
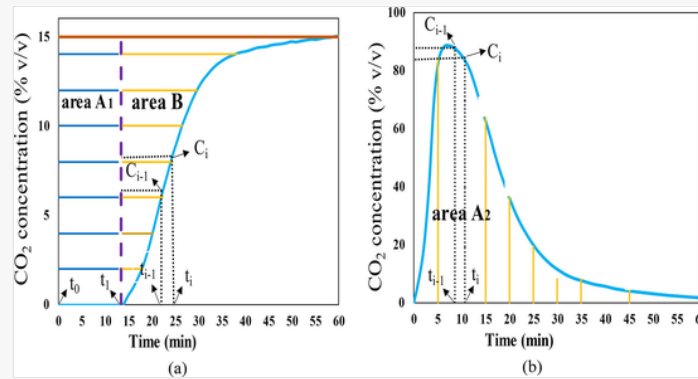
Graphical representation of the quantitative analysis performed for each cycle: (a) $CO_2$ adsorbed and (b) regenerated.

A blank test was performed with an empty reactor. The result obtained from the blank was subtracted from the retained ($q_{ret}$) and removed ($q_{rem}$) $CO_2$ obtained in Eqs. (3) and (4) to correct for the actual amount captured and regenerated, giving the mass of $CO_2$ adsorbed. The dynamic $CO_2$ capture capacity of the adsorbent was then calculated by the following expression:

$$q_{CO_2} = \frac{m_{CO_2}}{m_{ad}} \tag{5}$$

where $q_{CO2}$ is the $CO_2$ capture capacity (mg $CO_2$/g of adsorbent), $m_{CO2}$ is the mass of $CO_2$ adsorbed (mg) and $m_{ad}$ is the mass of adsorbent used (g).
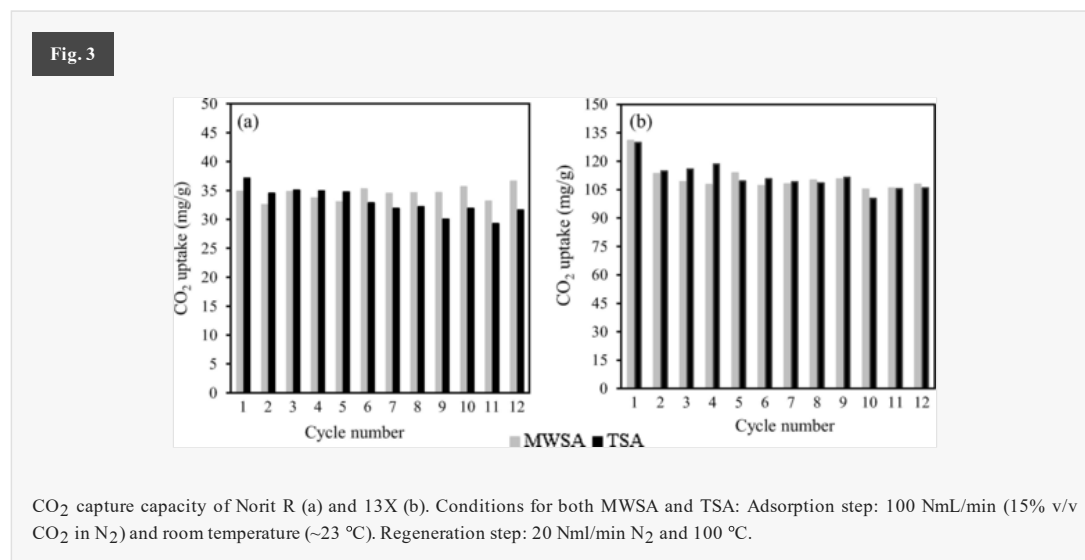
Power consumed during the regeneration of the adsorbents was measured and compared for MWSA and TSA. In the MWSA, the microwave power was recorded online with a 660 Touch Control Terminal (P/N TER6605G) which acted as the working interface for the microwave apparatus. In the TSA, power consumption was measured with a plug-in energy saving power meter (ENER007) from Energenie, however the consumed electrical energy was recorded online as volts by RS PRO IDM73 Handheld Digital Multimeter. Calibration curves were created for converting data from volts (V) to power (W) using ENER007 vs IDM73 plots. Then, the average power was calculated by multiplying the average heating power by the heating time. The average value of the first three cycles was taken to account for any small variations between cycles.

# 3 Results and discussion on dynamic $CO_2$ capture experiments: Microwave and thermal swing adsorption (MWSA & TSA) cycles

### 3.1 $CO_2$ adsorption capacity in MWSA and TSA cycles

Two of the key criteria in the selection of an industrially appropriate adsorbent for carbon dioxide capture are stability and durability after cycles. The adsorbent must sustain structural integrity with minimal effect on the capture capacity in a multi-cyclic process. It is not cost-effective to maintain a capture process with a non-durable material that needs a high adsorbent makeup rate. Mechanically unstable adsorbents may suffer from particle attrition by abrasion. High particle attrition leads to particle loss, unstable bed behaviour, particles being carried downstream causing plugging and the need for additional filtration components.

Accordingly, a decrease in the gas uptake over the cycles (provided that the same extent of regeneration is achieved within the regeneration method in all cycles) would indicate a change in the adsorbent after use, and consequently a compromise in the stability during and after operation. The latter may be explained by the effect on the adsorbent stability of the regeneration method employed, for instance, changes in the adsorbent structure (structural annealing), pore blockage, or formation of stable components onto pores [24]. The $CO_2$ adsorption capacities of Norit R and 13X during 12 consecutive cycles (note that every cycle is composed of an adsorption and a regeneration step) with MWSA and TSA are shown in Fig. 3.



Fig. 3

$CO_2$ capture capacity of Norit R (a) and 13X (b). Conditions for both MWSA and TSA: Adsorption step: 100 NmL/min (15% v/v $CO_2$ in $N_2$) and room temperature (~23 °C). Regeneration step: 20 Nml/min $N_2$ and 100 °C.

Regeneration conditions were identical for both MWSA and TSA (100 °C, 20 Nml/min $N_2$). It can be observed from Fig. 3(a) that Norit R presents stable $CO_2$ capture capacity behaviour during 12 cycles (33–36 mg/g) when regenerated with microwaves, whereas a drop in the capture capacity is observed after cycle 5 when regenerated with conventional heating (1.9 mg/g drop from cycle 5 to 6). Consequently, the average capture capacity of Norit R under selected conditions was found higher for MWSA (34.9 mg/g) than for TSA (31.4 mg/g) after cycle 5. Additionally, the variability encountered in the capture capacity in the rest of the cycles (34.66 ± 1.13 mg/g, average ± standard deviation) was found reasonable considering the variation in ambient temperature (23.88 ± 0.33 °C) during the adsorption step from one cycle to another (adsorption temperature varied from 22 to 25 °C).

Fig. 3(b) shows the MWSA and TSA cycles measured for 13X. A rather stable adsorption capacity throughout cycles 2 to12 (109.5 ± 2.68 mg/g in MWSA and 110.1 ± 4.90 mg/g in TSA, excluding cycle 1) with both regeneration methods is observed. As expected, the capacity dropped after the first cycle in both cases, from 131.0 to 113. mg/g in MWSA and 129.8 to 114.9 mg/g in TSA. The higher capture capacity measured in cycle 1 is due to the pre-clean and fully degassed sample (at 300 °C overnight). The subsequent cycles however presented a lowered capture capacity as

full regeneration was not achieved in cycle 1 under the selected operating conditions, but uptake capacity remained relatively steady from cycle 2 to 12, which indicates regeneration consistency throughout the cycles under the selected regenerating conditions. The lower standard deviations in MWSA also suggest a slightly steadier uptake capacity between cycles in MWSA compared to TSA.

The differences between $CO_2$ uptakes measured with MWSA and TSA are minimum for 13X compared with that found for Norit R (cycle 6 to 12). 13X zeolite is mainly composed of aluminosilicate which has a low dielectric response (almost transparent to microwaves), however the silica bonds at the surface are terminated in hydroxyl groups (silanols) have good microwave absorbing ability [25]. During MWSA, the silanols coupled with the electromagnetic radiation creating a heat flow from the surface into the bulk of the material. This is very much analogous to conventional heating (TSA) with the same type of heat flow gradient, which explains why the MWSA and TSA results are very similar (Fig. 3(b)). Additionally, 13X has $Na^+$ in its super-cages, which as suggested by McDowell, are responsible for absorbing most of the microwave radiation in faujasite and create thermal heat by rattling in the cages [26]. A study done by Whittington and Milestone on microwave heating of zeolites has found that 13X was heated to a greater extent when dry, compared to other types of zeolites with which the temperature rise was much faster under wet conditions. This is because $Na^+$ cations are driven out of the super-cages by the presence of water, decreasing their number in those sites and leading to reduced microwave absorption, hence lower temperature rise [27]. In this study, the 13X zeolite was fully degassed prior to the experiments and therefore considered dry. Based on the above theory, a rapid temperature rise was expected (200 °C /min) during adsorbent regeneration in the cyclic operations, however it took 7 mins (see Fig. 5d−f) for the zeolite to reach 100 °C from ambient temperature, corresponding to 10.7 °C /min heating rate. This can be attributed to the lack of rapid heating obtained with the lower average power applied (205 W) compared to the above-mentioned study (700 W), which may be below the power threshold required to achieve quick microwave absorption by the ions. The initial 7 mins heating time and 205 W power (i.e. 4100 kJ/kg) in the zeolite are 3.5 and 4.5 times of the heating time and power requirement in the activated carbon respectively, which needed 2 min and 46 W (i.e. 920 kJ/kg). Yet, the activated carbon achieved full regeneration while the zeolite did not, suggesting that Norit R has a much better thermal response to microwave heating than 13X in their dry pre-cleaned form. The lack of full regeneration in 13X can also be linked to its textural properties. 13X presents micropores of a smaller average diameter (0.46 nm) compared to Norit R (0.96 nm). Regenerating $CO_2$ in narrower micropores requires more energy. This is due to the greater forces of attraction experienced by the molecules due to the overlapping potential energy of the opposite pore walls. Adsorption energy increases with a decrease in pore size, and as a consequence, higher desorption energy is necessary when removing species adsorbed in such pores. The possibility of carbonate formation due to the interaction between the adsorbed $CO_2$ and the alkali cations ($Na^+$) in the zeolite has also been reported [28]. These carbonates were found to be stable even at temperatures of 700 °C. As described by Gallei and Stumpf, the formation of the carbonates involves three steps. First, the $CO_2$ is polarised when it contacts with the cation. Then, the carbon atom forms a bond with the oxygen atom bridging the silicon and aluminium atoms in the zeolite structure. Finally, the oxygen aluminium bond breaks, resulting in the formation of stable carbonate species [29]. The un-regenerated carbonate species formed in cycle 1 might also limited the accessibility of some adsorption sites by the $CO_2$, leading to a reduction in the uptake in subsequent cycles.

## 3.2 $CO_2$ regeneration in MWSA and TSA cycles

The efficacy of the adsorption process and the ability to tolerate repeated cycling are key criteria in establishing an industrial carbon dioxide capture process. Equally important are also the regeneration kinetics and the required regeneration energy. The regeneration kinetics impacts the cycle time (adsorption and regeneration time), hence the productivity of the separation process, and the quantity of adsorbent needed. Adsorbents with fast adsorption kinetics normally yield to a sharp breakthrough curve with a short distance between the breakthrough time and the saturation time. The intrinsic adsorbate-adsorbent interaction, as well as gas diffusion and mass transfer resistance play a crucial role in regeneration kinetics. Similarly, since adsorbent regeneration is an endothermic process involving an external energy input, the regeneration energy is a paramount factor in the viability of the capture process and has big implications on the running cost of the power plant. Both factors also affect the regeneration extent, regeneration time and breakthrough time. With this in mind, data for adsorption and regeneration of Norit R and 13X for twelve consecutive MWSA and TSA cycles, including breakthrough times and the time required to achieve different extents of regeneration (80, 90 and 100%) were determined and presented in the following subsections.

### 3.2.1 Regeneration extent

From Table 1, it is observed that Norit R presents practically the same breakthrough times with both TSA and MWSA, and they are consistent across the 12 cycles tested ($t_b$ = 5.3 min). On the other hand, the breakthrough times measured with 13X vary within cycles and on average are approximately one minute shorter in MWSA cycles compare to TSA cycles.

Table 1

**Q12** $CO_2$ adsorbed and regenerated, breakthrough time and time at which the 80, 90 and 100% of regeneration is achieved for 12 TSA and MWSA cycles.

| Cycle Number | | | 1 | 2 | 3 | 4 | 5 | 6 | 7 | 8 | 9 | 10 | 11 | 12 | $\bar{x} \pm SD$ |
|---|---|---|---|---|---|---|---|---|---|---|---|---|---|---|---|
| Norit R | MWSA | $T_{ads}$ | 23.0 | 24.0 | 25.0 | 25.0 | 24.0 | 23.0 | 24.0 | 24.0 | 24.0 | 24.0 | 24.0 | 24.0 | $24.0 \pm 0.6$ |
| | | $q_{ad}$ | 34.8 | 32.5 | 34.8 | 33.7 | 33.0 | 35.3 | 34.5 | 34.6 | 34.6 | 35.6 | 33.1 | 36.6 | $34.4 \pm 1.1$ |
| | | $t_b$ | 5.3 | 5.3 | 5.3 | 5.3 | 5.3 | 5.3 | 5.3 | 5.3 | 5.3 | 5.3 | 5.3 | 5.3 | $5.3 \pm 0.0$ |
| | | $q_{re}$ | 32.7 | 32.1 | 31.6 | 30.8 | 32.3 | 33.0 | 33.0 | 32.7 | 31.5 | 31.5 | 32.9 | 32.6 | $32.2 \pm 0.7$ |
| | | $t_{80}$ | 18.0 | 19.1 | 18.0 | 18.0 | 17.0 | 18.0 | 18.0 | 18.0 | 17.0 | 17.0 | 18.0 | 18.0 | $17.8 \pm 0.6$ |
| | | $t_{90}$ | 22.3 | 23.3 | 23.3 | 22.3 | 21.2 | 22.3 | 22.3 | 22.3 | 21.2 | 21.2 | 22.3 | 22.3 | $22.2 \pm 0.7$ |
| | | $t_{100}$ | 40.3 | 41.4 | 41.4 | 40.3 | 39.3 | 40.3 | 40.3 | 40.3 | 39.3 | 39.3 | 40.3 | 40.3 | $40.2 \pm 0.7$ |
| | TSA | $T_{ads}$ | 23.5 | 23.6 | 24.0 | 24.6 | 23.0 | 22.0 | 23.0 | 24.0 | 25.0 | 25.0 | 25.0 | 25.0 | $24.0 \pm 1.0$ |
| | | $q_{ad}$ | 37.1 | 34.5 | 35.1 | 34.9 | 34.7 | 32.8 | 31.9 | 32.2 | 30.0 | 31.9 | 29.3 | 31.6 | $33.0 \pm 2.2$ |
| | | $t_b$ | 5.3 | 5.3 | 5.3 | 5.3 | 5.3 | 5.3 | 5.3 | 5.3 | 5.3 | 5.3 | 5.1 | 5.3 | $5.3 \pm 0.1$ |
| | | $q_{re}$ | 33.7 | 33.2 | 33.3 | 32.7 | 34.0 | 33.3 | 32.2 | 32.4 | 31.9 | 32.4 | 31.3 | 30.8 | $32.6 \pm 0.9$ |
| | | $t_{80}$ | 13.8 | 13.8 | 13.8 | 14.9 | 13.8 | 13.8 | 13.8 | 13.8 | 13.8 | 13.8 | 13.8 | 13.8 | $13.9 \pm 0.3$ |
| | | $t_{90}$ | 18.0 | 18.0 | 18.0 | 19.1 | 18.0 | 17.0 | 17.0 | 17.0 | 17.0 | 18.0 | 18.0 | 17.0 | $17.7 \pm 0.6$ |
| | | $t_{100}$ | 32.9 | 32.9 | 32.9 | 34.0 | 31.8 | 31.8 | 31.8 | 31.8 | 31.8 | 32.9 | 32.9 | 31.8 | $32.4 \pm 0.7$ |
| 13X 13X | MWSA | $T_{ads}$ | 24.0 | 24.0 | 25.0 | 26.0 | 27.0 | 27.0 | 26.0 | 27.0 | 24.0 | 24.0 | 24.0 | 24.0 | $25.2 \pm 1.3$ |
| | | $q_{ad}$ | 131.0 | 113.4 | 109.2 | 107.6 | 113.8 | 107.2 | 107.9 | 109.9 | 110.6 | 105.2 | 105.7 | 107.8 | $110.8 \pm 6.9$ |
| | | $t_b$ | 15.9 | 14.8 | 14.8 | 13.8 | 15.9 | 14.8 | 14.8 | 14.8 | 15.9 | 13.8 | 14.8 | 12.7 | $14.7 \pm 0.9$ |
| | | $q_{re}$ | 96.6 | 90.1 | 89.5 | 98.0 | 95.0 | 92.5 | 95.7 | 86.5 | 90.8 | 92.7 | 90.4 | 92.6 | $92.5 \pm 3.2$ |
| | | $t_{80}$ | 28.6 | 29.7 | 30.8 | 30.8 | 31.8 | 28.6 | 29.7 | 29.7 | 28.6 | 27.6 | 30.8 | 26.5 | $29.4 \pm 1.5$ |
| | | $t_{90}$ | 40.3 | 42.4 | 44.6 | 44.6 | 45.6 | 41.4 | 42.4 | 43.5 | 41.4 | 38.2 | 43.5 | 39.3 | $42.3 \pm 2.2$ |
| | | $t_{100}$ | 84.9 | 91.2 | 94.4 | 94.4 | 98.7 | 90.2 | 92.3 | 93.4 | 89.1 | 83.8 | 94.4 | 87.0 | $91.2 \pm 4.2$ |
| | TSA | $T_{ads}$ | 22.4 | 23.9 | 23.9 | 24.0 | 25.0 | 25.0 | 25.7 | 26 | 25.5 | 24.9 | 26.9 | 27.0 | $25.0 \pm 1.3$ |
| | | $q_{ad}$ | 129.8 | 114.9 | 115.9 | 118.5 | 109.5 | 110.7 | 109.1 | 108.7 | 111.6 | 100.5 | 105.5 | 105.9 | $111.7 \pm 7.2$ |
| | | $t_b$ | 17.0 | 17.0 | 17.0 | 17.0 | 15.9 | 15.9 | 15.9 | 15.9 | 15.9 | 14.8 | 15.9 | 15.9 | $16.2 \pm 0.7$ |
| | | $q_{re}$ | 101.7 | 104.4 | 102.8 | 104.3 | 100.0 | 100.1 | 103.3 | 99.8 | 101.7 | 98.5 | 98.3 | 97.4 | $101.0 \pm 2.3$ |
| | | $t_{80}$ | 26.5 | 26.5 | 25.5 | 25.5 | 25.5 | 24.4 | 25.5 | 24.4 | 25.5 | 24.4 | 24.4 | 24.4 | $25.2 \pm 0.8$ |
| | | $t_{90}$ | 37.1 | 36.1 | 36.1 | 36.1 | 36.1 | 36.1 | 36.1 | 35.0 | 36.1 | 35.0 | 35.0 | 35.0 | $35.8 \pm 0.6$ |
| | | $t_{100}$ | 63.7 | 65.8 | 62.6 | 65.8 | 64.7 | 63.7 | 64.7 | 62.6 | 63.7 | 63.6 | 63.7 | 64.7 | $64.1 \pm 1.0$ |

Notes:

$T_{ads}$ = adsorption temperature (°C).

$q_{ad}$ = amount adsorbed per gram of adsorbents (mg/g).

$q_{re}$ = amount regenerated per gram of adsorbents (mg/g).

$t_b$ = breakthrough time (min) at $\frac{outlet concentration (C)}{inlet concentration (C_0)} = 0.05$.

$t_{80}$, $t_{90}$ and $t_{100}$ = time (min) at which the regeneration percentage achieved is 80, 90 and 100%, respectively.

$x \pm SD$ = Mean ± Standard Deviations.

The regeneration percentages of cycles 2, 6 and 12 are depicted in Fig. 4(a–f). The time taken to regenerate 80, 90 and 100% of the total amount desorbed was compared for TSA and MWSA for the selected adsorbents (Fig. 4 and Table 1

). The heating period required to regenerate each of the above-mentioned percentages was found to be less in all cases with TSA.
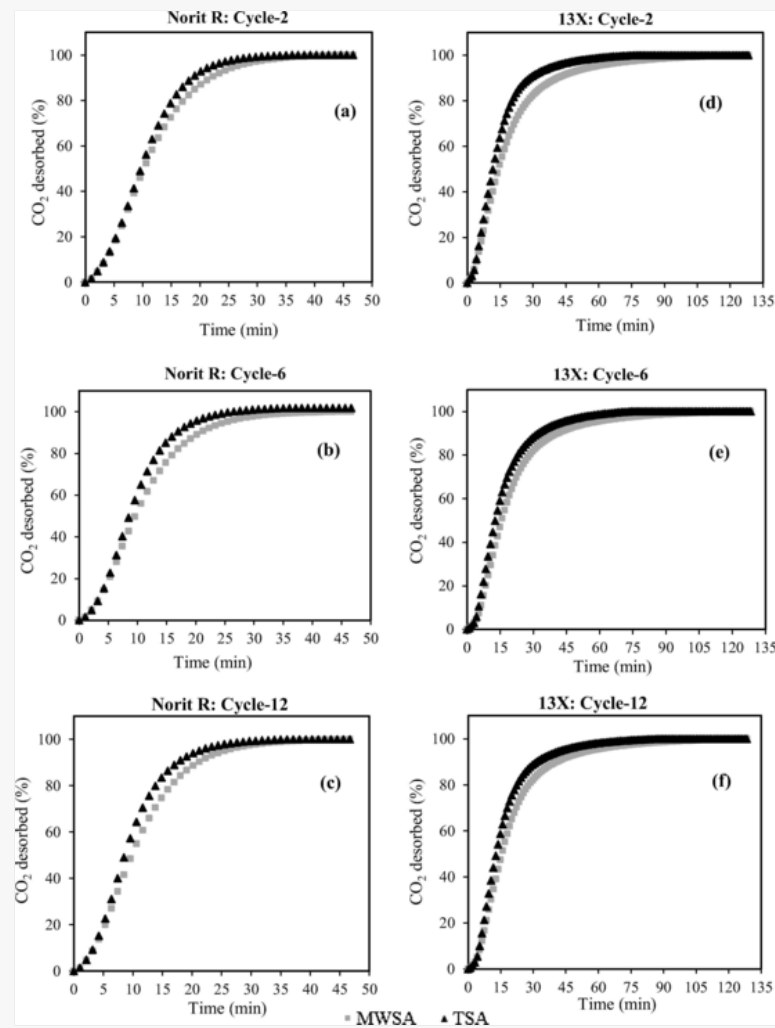


Percentage of $CO_2$ regenerated at each point out of the total desorbed by the end of the heating period of Norit R (cycle 2 (a), cycle 6 (b), cycle 12 (c)) and 13X (cycle 2 (d), cycle 6 (e), cycle 12 (f)) for TSA and MWSA.

Norit R exhibits overlapping regeneration percentage profiles in the first 2 min, achieving the 5% regeneration in the first 2 mins in all plotted cycles with both TSA and MWSA. After that, regeneration percentage is always found slightly higher with TSA for the same total heating period of 47 mins until completion. The difference in the regenerated percentage between TSA and MWSA is highest at approximately minute 15th. From min 37th of heating time, samples achieved over 99% regeneration in both heating modes in all cycles. From that point, all curves overlap with the formation of a plateau until completion. This indicates that in the last 10 mins of the regeneration, less than 1% of the total adsorbate is desorbed.

Over 50% of regeneration was achieved after 10 mins of heating for both regeneration methods. With Norit R, it took 17.7, 13.9 and 32.4 mins on average, to achieve 80, 90 and 100% regeneration, respectively. Those times increased by 4.0, 4.5 and 7.8 mins (average) with MWSA in the order mentioned. A similar trend was observed in 13X with regeneration percentage being higher for TSA than MWSA for the same regeneration time, except for the 1st min where regeneration percentage achieved with both regeneration strategies overlap. Achieving 50% of regeneration in 13X took 3.2 mins more in MWSA at 15.9 mins compared to the 12.7 mins in TSA. The regenerated percentage in cycle 2 is double (10%) that of cycles 6 and 12 (5% in both cycles) after 4 mins of heating for both regeneration strategies. This indicates that in cycle 2, the amount removed at the beginning of the regeneration process is higher in proportion to the total removed, compared to the other cycles. This is most likely rooted in the large amount of $CO_2$ retained from the high adsorption capacity in cycle 1, desorbing in cycle 2. A difference in the percentage of regeneration between TSA and MWSA commenced after 4 mins of heating in all cycles, but it is more pronounced in cycle 2. For 13X, 25.3 and 35.8 mins on average are required with MWSA to achieve 80 and 90% regeneration, respectively. These are longer heating times (by 4.2 and 6.5 mins, respectively) than those needed with TSA to achieve the same regeneration percentages. To achieve 100% regeneration in 13X, 64.1 mins with TSA and 91.2 mins with MWSA on average were needed.

Note (Table 1) that there are a number of cycles where the regenerated amount is greater than that captured (i.e. $q_{re} > q_{ad}$) in the same cycle. The origin of such a discrepancy could be data evaluation errors (overestimation/underestimation of the areas above and under the curves), as well as variability in the amount of $CO_2$ regenerated from cycle to cycle, resulting in an amount retained on the adsorbent. For example, incomplete regeneration in cycle 2 could lead to proportionally lower capture capacity in cycle 3, but if the residual $CO_2$ plus the added $CO_2$ are regenerated in cycle 3, the capacity in the next cycle 4 will be higher than in cycle 3. Such a result is not uncommon in the literature for cyclic tests [11].

### 3.2.2 Regeneration kinetics

The rate of adsorbate desorption in any swing adsorption process is an essential parameter in evaluating the efficiency of the adsorbent. Slow desorption kinetics leads to increased desorption times and a comparatively reduced number of swing cycles for a given separation time. It also influences the amount of adsorbent needed for the separation process, as a faster desorption rate allows for more intense or frequent use of the adsorbent, so larger quantities of adsorbate can be separated. The Regeneration Rate (RR, in mg $CO_2$ desorbed / min) is defined by the following expression:

$$RR = \Delta m / \Delta t \tag{6}$$

where $\Delta m$ (mg) is the change in mass of desorbed gas during regeneration (amount of gas released during the fixed time interval between two consecutive measurements), and $\Delta t$ (min) is the change in regeneration time (the fixed time interval between two consecutive measurements).

In any regeneration process, the profile of the adsorbate regeneration rate is mainly affected by the regeneration temperature and the total flow rate of the sweeping gas. The latter assists the regeneration process by facilitating the movement of the adsorbate from the adsorbent near to the bed exit. In this study the desorption rates were evaluated by maintaining both the regeneration temperature and the total sweeping gas flow rate constant (100 °C and 20 NmL/min of $N_2$, respectively). Results were compared for the two regeneration strategies employed: MWSA and TSA. Fig. 5 presents the regeneration rate along with the regeneration temperatures of Norit R and 13X (few cycles plotted) with MWSA and TSA.

Fig. 5
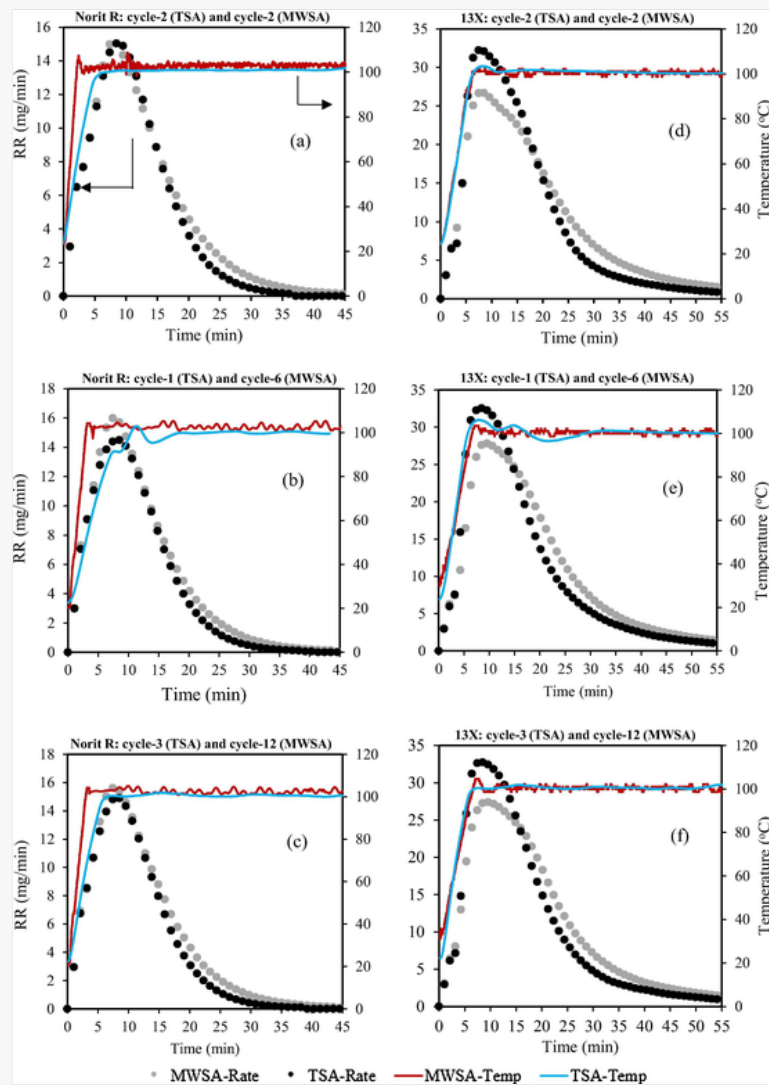
CO$_2$ regeneration rate and regeneration temperature of Norit R (a, b, c) and 13X (d, e, f) in cycles 2, 1 and 3 for TSA and 2, 6, and 12 for MWSA.

For Norit R (Fig. 5a–c), the regeneration temperature was always achieved faster with MWSA compared to TSA (after 2 and 4 mins from the start of the regeneration step, respectively). Heating rates measured in the 2nd and 4th mins period with MWSA and TSA were 38 and 18 °C/min, respectively, twice as fast with MWSA than with TSA. The CO$_2$ desorption rate profiles overlap in most cycles for the first 15 mins of regeneration. Afterward, CO$_2$ desorption rate was found to be higher for MWSA than TSA.

Maximum desorption rates of 15.61, 16 and 15 mg/min are reached around 7.8 mins (average) after the start of the regeneration for MWSA (Fig. 5(a), (b) and (c). For TSA, on the other hand, desorption peak rates of 15, 14.5 and 14.9 mg/min are obtained around 8.5 mins (average) in Fig. 5(a), (b) and (c), respectively. On average, the regeneration rate reaches a maximum of 15.5 mg/g with MWSA compared to 14.8 mg/g with TSA due to the higher desorption rate found with microwave heating (Fig. 5b). The regeneration profile follows two distinct stages after the maximum: between minutes 9th and 18th it shows a sharp decreasing slope, followed by a slower regeneration step from minute 18th until the end. However, it is worth noting the difference observed in desorption rates in the final part of the profiles, this time being greater for MWSA than for TSA, which suggests faster CO$_2$ desorption rates in the later stages of the regeneration, when performed with microwave heating.

In the case of 13X (Fig. 5d–f), the regeneration temperature was reached after 7 mins of initiating regeneration in both TSA and MWSA. This is equivalent to 10 °C/min. It was observed that both MWSA and TSA presented similar desorption rates in the first 5 mins of the regeneration, however the CO$_2$ desorption rate profiles are evidently dissimilar thereafter. The maximum rate of desorption was achieved after 7.5 mins in all cases, but it is clearly higher for TSA (32 mg/min) than for MWSA (27 mg/min). After the maximum desorption rate, the desorption rate profile follows three paths in MWSA. An initial slower decline (from minutes 9th to 17th) with an average CO$_2$ desorption rate of 25.12 mg/min, followed by a second step (from minutes 18th to 35th) with a slower desorption rate at an average of 11.14 mg/min. From minute 36th to the end, the slope of the profile becomes somewhat flatter with an average desorption rate of 2.49 mg/min. The regeneration rate profile using TSA after the maximum can be split into two regions: a region with a steeper slope (from minutes 9th to 29th) where the average CO$_2$ desorption rate is 17.42 mg/min, and the last part (minute 30th to end) where the average desorption rate is 2.0 mg/min.

These observations reveal that in the case of 13X, for the same sample thermal response (see the overlap in temperature profiles exhibited with both heating sources), $CO_2$ is desorbed faster with conventional heating than with microwave heating for the first 16 mins (average calculated for the 3 cycles plotted in Fig. 5d–f), and it then becomes faster using MWSA from minute 16th until the end of regeneration (not fully achieved after 55 mins). It is noteworthy to mention that this result is contrary to our initial hypothesis on the behaviour of 13X with MWSA, which was based on the generally held view of microwave heating leading to faster adsorbate removal, hence higher regeneration rates. Nonetheless, it is in-line with a recently reported article by Cherbanski [11] where similar desorption profiles were observed when the heating powers in MWSA and TSA were matched. As explained in Section 3.1, the main heating mechanism which takes place when microwaves are applied to 13X is via ionic conduction of $Na^+$. A conceivable theory to explain the lower $CO_2$ desorption rate in 13X observed with microwave heating is the possibility of $Na^+$ hindering the $CO_2$ molecules attempting to migrate through the small pores of the adsorbents during heating. When the external electromagnetic field is applied, the $Na^+$ cations are induced to move through the zeolite structure or rattle in the cages [26]. It is proposed that the average power used in this study is too low to cause rapid ionic conduction/rattling but sufficient to create ionic movements to help reach the target temperature. It is proposed that slow moving $Na^+$ cations having a hindering effect on the pace at which $CO_2$ diffuses out from and through small pores. In Fig. 5(b, c, e and f), dissimilar cycles of TSA and MWSA are compared. This was carried out to determine whether the shape of rate profiles is maintained or changed with the progression of cyclic operation, especially in the MWSA. This also allows a determination of the existence of any dissimilarity in rate profiles from (a) and (d) where matching cycles are compared.

### 3.2.3 Regeneration efficiency after cycles

If a regenerated sample sustains lower or higher uptake than that of the fresh (unused) sample in repeated cycles, the cause is most likely rooted in the regeneration conditions as well as method. Accordingly, Regeneration Efficiency (RE, in %) was used to evaluate the ability to maintain the original adsorption capacity of the adsorbents during repeated cycles, and was calculated by using the following equation:

$$RE = (q_i/q_0) \cdot 100 \qquad (7)$$

where $q_0$ is the $CO_2$ capture capacity obtained in the first cycle (fresh adsorbent) and $q_i$ is the $CO_2$ capture capacity of each individual cycle (from 2nd to i[th]) [30].

Fig. 6 represents the RE calculated for Norit R and 13X with MWSA and TSA, respectively. Fig. 6(a and c) are evaluated with cycle 1 included in the calculation (i.e. $q_0$ = capacity of cycle 1, the fresh sample), where in (b & d) cycle 1 is disregarded (i.e. $q_0$ = capacity of cycle 2).



Fig. 6
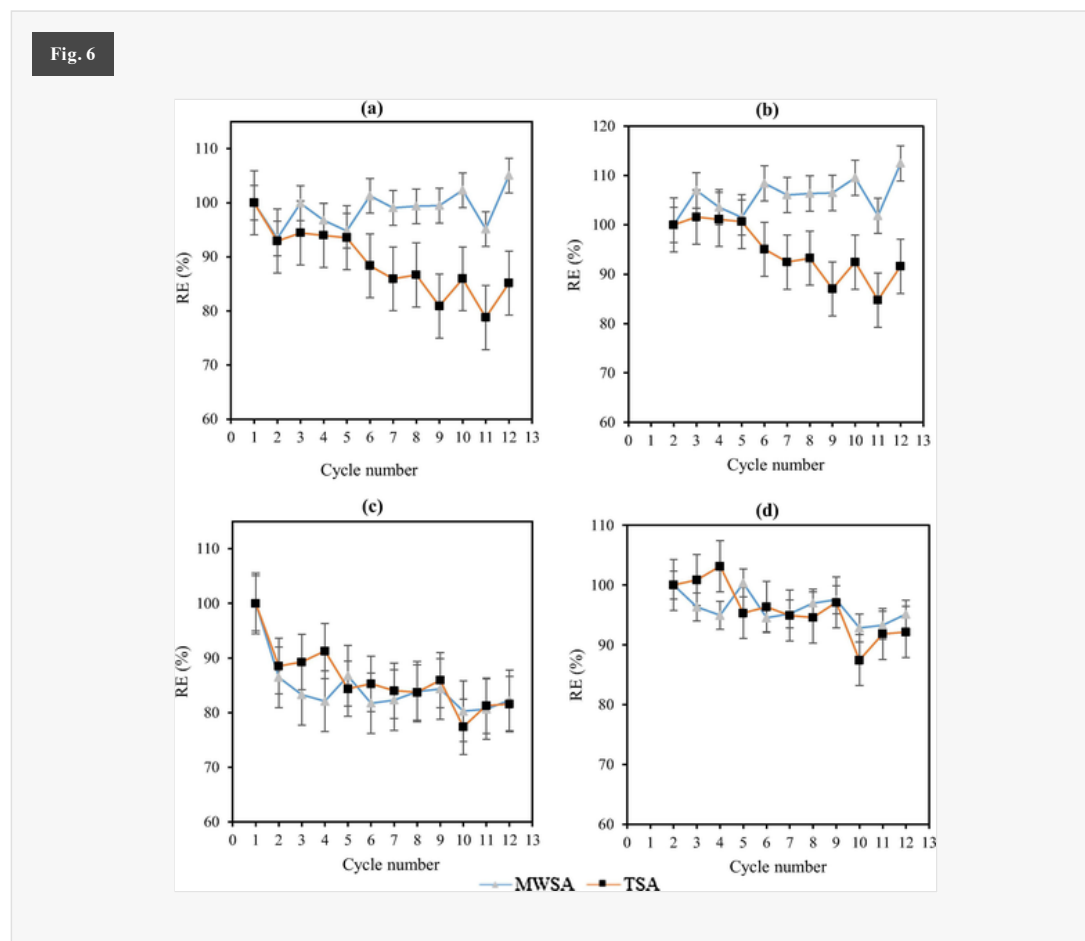
The RE obtained for Norit R with TSA cycles ranged from 78.78 to 94.43%, and exhibits slight oscillations from one cycle to another, which are within ±6.19 SD of the average RE. A 7% drop in RE from cycle 1 to cycle 2 is observed, and a constant RE value (average RE = 93%) achieved in the next four consecutive cycles. After cycle 5, a decreasing trend was observed in RE values up to cycle 8, after which RE value presents small fluctuations with an average RE of 84.5%.

The average, maximum and minimum RE observed with MWSA for Norit R are 99, 105 and 93%, respectively, when cycle 1 is included (Fig. 6a). On the other hand, when cycle 1 is disregarded, these are 105.7, 112.5 and 101.5% respectively (Fig. 6b). Larger capacity observed in some later cycles than in cycle 1 (Fig. 6a) or cycle 2 (Fig. 6b) led to RE values larger than 100% in the relevant cycles.

The above demonstrates consistency regarding the level of capture capacity achieved in each cycle under the selected regeneration conditions and retained sample properties after microwaving. In the case of TSA, RE values dropped by 8.5% from cycle 5, which indicates less stability in the CO$_2$ capture capacity after cycles compared to MWSA. Therefore, it can be concluded that the activated carbon showed great stability during MWSA as the steady state was reached relatively soon for the cycles measured. Comparing the effect of the regeneration strategies employed, results obtained with Norit R show that microwave-assisted regeneration (MWSA) was more successful than regeneration assisted with conventional heating (TSA) under the conditions tested, as it led to a more stable uptake capacity as well as higher RE efficiency. It also resulted in a slightly higher CO$_2$ desorption rate in the later stages of the heating.

The relatively low desorption temperature selected for this study means that the cause of the RE decrease observed with TSA cycles for Norit R is unlikely to be due to adsorbent structural changes, but rather, incomplete regeneration achieved with conventional heating in the first 5 cycles where the retained (residual) CO$_2$ affected adsorbent capacity in the subsequent cycles (see also Table 1). Based on the RE results shown in Fig. 6a, it can be concluded that for the selected experimental conditions, regeneration with microwave heating (MWSA) is superior to conventional heating (TSA) for Norit R, and that a consistent, full regeneration in multi-cycle operation is guaranteed with the former type of regeneration.

In the case of 13X, RE dropped by over 10% after the first regeneration (Fig. 6c), after which it was maintained at 83.1 ± 3.2% and 84.8 ± 6.9% with MWSA and TSA, respectively. As explained in Section 3.1, the most probable cause of this drop is the regeneration temperature and power output selected (probably insufficient to allow for complete regeneration). However, RE stabilises from cycle 5 (RE average approximately 82%) with both regeneration techniques.
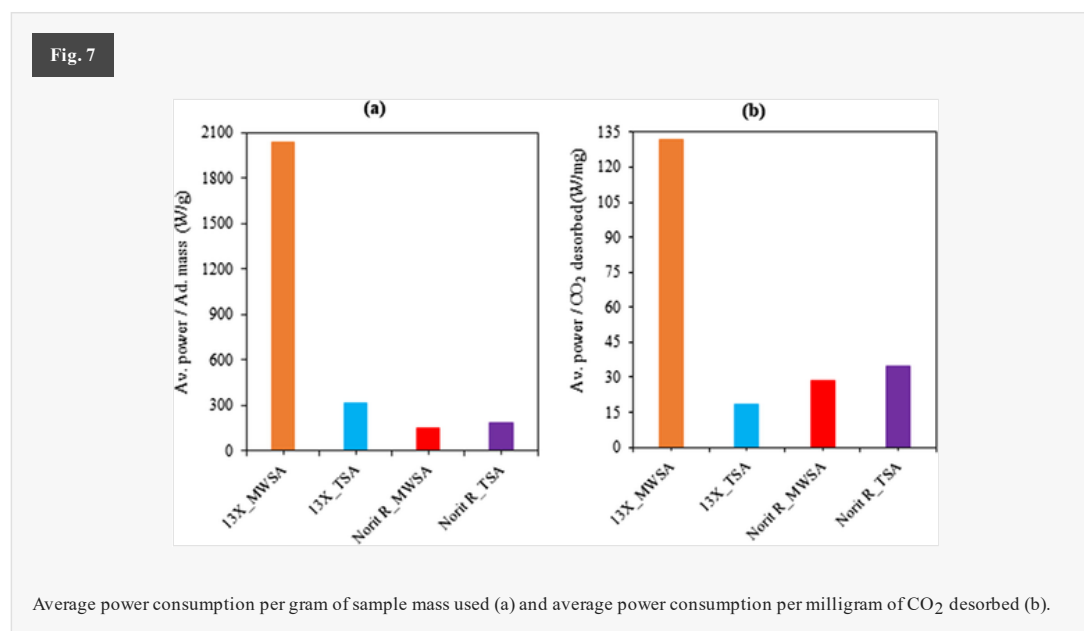
Taking cycle 2 as the reference (i.e. $q_0$) (Fig. 6b and d), RE data was analysed to discard major differences due to the unrepresentative fresh sample used in every first cycle and obtain a closer picture of what the continuous separation process would be like in practice (cycle 1 is not considered). For both adsorbents, the trend was unaffected, however, the minimum, maximum and average RE have all increased. The increase is particularly marked for 13X where RE raised by more than 10% for both heating methods. For instance, with TSA the minimum, maximum and average RE increased from 77.4, 91.3 and 83.1%, to 87.4, 103 and 95.8% where with MWSA it raised from 80.2, 86.7 and 84.8% to 92.8, 100.3 and 96.15%, respectively. This reveals that if the initial cycle is disregarded, 13X is in fact working within RE ± 9% and RE ± 5% in TSA and MWSA, respectively.

In line with the information presented in Section 3.1, RE results support the view that Norit R maintained a more stable and predictable performance under MWSA than TSA over the cycles conducted. With 13X nevertheless, similar regeneration efficiency was achieved with both TSA and MWSA.

### 3.2.4 Regeneration energy

The microwave and electrical power consumed in MWSA and TSA, normalised by the sample mass (specific regeneration energy), are depicted in Fig. 7a. The results show very different energy consumption behaviour by the two samples. The power per gram consumed in regenerating the activated carbon is 1.22 times higher in TSA than MWSA (i.e. 152.45 vs 187.50 W/g). Additionally, the lowest specific regeneration energy (or lowest power consumption per unit mass) is observed with Norit R in MWSA. On the other hand, the highest specific power consumption was recorded for 13X in MWSA. The amount of microwave power spent in regenerating a gram of the zeolite in MWSA is 6.50 times higher than the electrical power spent in TSA (i.e. 2035.12 vs 314.17 W/g). The normalised spent power (W) per unit mass of CO$_2$ desorbed (mg) is shown in Fig. 7b. The highest values are seen with 13X in the MWSA process whereas the lowest is observed for the same adsorbent but in the TSA process. The power used in removing a milligram of adsorbate (i.e. CO$_2$) is 7.10 times bigger in the MWSA than in TSA for 13X. On the other hand, it is 1.22 times bigger in TSA than in MWSA for Norit R. Comparing power consumption between the two adsorbents for the same heating mode, 13.35 times more power is needed to regenerate a gram of the zeolite in MWSA compared to the

activated carbon. In TSA, the difference is much smaller with only 1.68 times more power requirement for 13X than Norit R. Regarding power spent in removing a similar amount of $CO_2$ from both adsorbents, 4.65 times more power usage is observed with 13X than Norit R with microwave heating. With conventional heating, 1.85 times more power uptake is seen with Norit R than 13X.



Fig. 7

Average power consumption per gram of sample mass used (a) and average power consumption per milligram of $CO_2$ desorbed (b).

Overall, the results indicate that the behaviour of microwave power uptake is adsorbent dependent based on the material's dielectric properties. In these tests, microwave regeneration led to energy savings over conventional regeneration with the activated carbon, but it was not the case with the zeolite. It is, however, noteworthy to point out that two dissimilar energy forms are compared here. In MWSA, power is consumed in the form of microwave energy, whereas in TSA power is consumed in the form of electrical energy. In any case, the adsorbent's power uptake is reported here as obtained but is deemed inconclusive due to an inherent difference in the power demand between the two heating methods. This is because of a significant difference in the scale of the instruments used in supplying the power for heating up the adsorbents. In the MWSA system, the apparatus used was a multimode and heavy-duty professional microwave (FlexiWAVE, from Milestone) It has a large cavity volume (approximately 70.5 l) and consists of two magnetrons, capable of producing a total power output of 1900 W. On the other hand, the TSA system used consisted of a simple conductive heating source provided by an electric rope heater connected to a 240 V output (max) variable autotransformer (Variac). This resulted in disproportionally higher electric power demand in the MWSA, however, it is believed that the power consumption would be reduced in MWSA for both adsorbents if a comparable apparatus size is used for TSA. Studies are currently being conducted on the optimisation of the conventional heating system in a way that would lead to comparable electrical power used to draw a more fitting conclusion on the overall energy requirements of both thermal swing systems.

### 3.3 Dielectric properties of the adsorbents (fresh)

Since MWSA is one the regeneration strategy under investigation, information on the dielectric properties of the adsorbents employed assists in understanding the interaction between the adsorbents and the electromagnetic field (microwave radiation). This includes expected dielectric heating performance as well as potential thermal runaway. For that reason, the dielectric properties of Norit R and 13X were measured using the resonant cavity perturbation technique while heating samples from 20 to 500 °C at 5 °C/min heating rate. Table 3 shows the dielectric constant ($\varepsilon'$) and loss factor ($\varepsilon''$) of Norit R and 13X.

In general, the dielectric properties of the two samples change with temperature quite differently. For Norit R, $\varepsilon'$ drops from 16.25 at 20 °C, to 15.36 at 50–100 °C, followed by a slow increase at higher temperatures. On the other hand, $\varepsilon''$ displays a changing value oscillating between a maximum value of 0.07 at 200 °C and a minimum value of 0.03 at 450 °C. It shows very little dependence on the temperature change. The overall trending line of the data is almost flat. Contrarily, for 13X the two parameters, $\varepsilon'$ and $\varepsilon''$, are affected by temperature in a similar mode. Initially, they both fell between 20 and 50 °C then increased until reached 100 °C for $\varepsilon'$ and 150 °C for $\varepsilon''$, before falling to their smallest values ($\varepsilon' = 2.46$ at 300 °C and $\varepsilon'' = 0.73$ at 200 °C). From the minimum, both parameters rise continuously for the temperature presented.
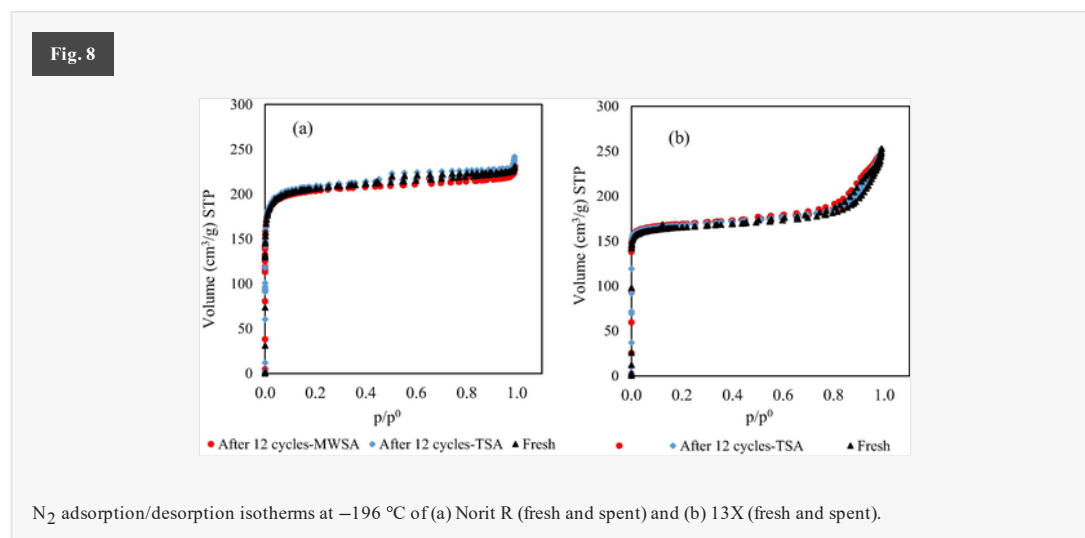
In terms of microwave application, the slow change of $\varepsilon'$ and the oscillating $\varepsilon''$ in Norit R yield a loss tangent (tan $\delta = \varepsilon''/\varepsilon'$) that fluctuates slightly with the temperature increase. This keeps the temperature under microwave heating in check, where at certain temperatures the loss factor drops or increases, leading to a decline or rise of temperature ramp because of reduction or surge in heat dissipation from the material. In such cases, the temperature can be maintained within a pre-set value to reduce the undesired 'thermal runway effect'. For 13X, absorption of MW irradiation

decreased up to 300 °C due to the declining dielectric constant, nevertheless, the loss tangent increased in this region because of the overall upward trend of the loss factor. The loss factor continuously increased when the temperature raised from 300 to 500 °C. This could be that as the material structure of the zeolite expands under the heat, the ions responsible for temperature increase become freer as they acquire additional space to rattle around, which in effect leads to more temperature increase, hence a continuous effect.

Overall, from Table 3, it is observed that the activated carbon absorbs microwave energy better than the zeolite due to the higher value of dielectric constant recorded (over 4 times higher at 100 °C). On the other hand, the zeolite may convert the absorbed energy into heat better than the activated carbon due to the higher loss factor recorded. In this work, a faster temperature increase was observed in the activated carbons, indicating that for the low regeneration temperature employed, having higher energy absorbance over-outweighed than having a better conversion of absorbed microwave energy into heat.

### 3.4 Adsorbent stability after MWSA and TSA cycles: tTextural properties

Textural properties were evaluated for both fresh samples and those subjected to MWSA and TSA, in order to evaluate any changes due to continuous heating and cooling, and microwave radiation. The $N_2$ adsorption-desorption isotherms at −196 °C are displayed in Fig. 8. Table 2 summarises the adsorbent's textural parameters extracted from the $N_2$ adsorption isotherms. Norit R displays a type I isotherm in the IUPAC classification [21]. A sharp $N_2$ uptake at very low relative pressures ($p/p^0 < 0.1$) is observed, which is followed by a nearly horizontal plateau up to $p/p^0 = 0.4$. A hysteresis loop commences from $p/p^0 > 0.4$, indicating that capillary condensation took place into mesopores. The sharp uptake observed at low relative pressures is associated with the presence of microporous ($W_0 = 0.27$ cm$^3$/g), and the rather narrow hysteresis indicates the existence of a small volume of mesopores (0.007 cm$^3$/g). In the case of 13X, the $N_2$ adsorption isotherm exhibits a type IV isotherm, confirming the presence of mesopores ($V_{meso} = 0.092$ cm$^3$/g). The sharp uptake shown at $p/p^0 < 0.4$ also indicates the presence of a significant volume of micropores ($W_0 = 0.22$ cm$^3$/g).

**Fig. 8**



$N_2$ adsorption/desorption isotherms at −196 °C of (a) Norit R (fresh and spent) and (b) 13X (fresh and spent).

**Table 2**

> ⓘ The table layout displayed in this section is not how it will appear in the final version. The representation below is solely purposed for providing corrections to the table. To preview the actual presentation of the table, please view the Proof.

Temperature dependence of the dielectric constant ($\varepsilon'$) and loss factor ($\varepsilon''$) of Norit R and 13X.

| Temperature | Norit R | | 13X | |
|---|---|---|---|---|
| (°C) | $\varepsilon'$ | $\varepsilon''$ | $\varepsilon'$ | $\varepsilon''$ |
| 20 | 16.25 | 0.06 | 4.09 | 0.85 |
| 50 | 15.36 | 0.05 | 3.48 | 0.73 |
| 100 | 15.36 | 0.05 | 3.64 | 0.92 |
| 150 | 15.43 | 0.06 | 3.33 | 1.01 |
| 200 | 15.47 | 0.07 | 2.66 | 0.73 |
| 250 | 15.65 | 0.04 | 2.48 | 0.85 |
| 300 | 15.72 | 0.06 | 2.46 | 0.87 |
| 350 | 15.77 | 0.07 | 2.54 | 1.11 |

| 400 | 15.90 | 0.06 | 2.74 | 1.14 |
| 450 | 16.04 | 0.03 | 2.79 | 1.29 |
| 500 | 16.07 | 0.04 | 3.07 | 1.60 |

**Table 3**

> ⓘ The table layout displayed in this section is not how it will appear in the final version. The representation below is solely purposed for providing corrections to the table. To preview the actual presentation of the table, please view the Proof.

Textural parameters calculated from the $N_2$ isotherms at −196 °C.

| Sample | Sample condition | $S_{BET}$ (m²/g) | $p/p^0$ | $V_p$ (cm³/g) | $W_0$ (cm³/g) | $V_{meso}$ (cm³/g) | $D$ (nm) |
|---|---|---|---|---|---|---|---|
| Norit R | Fresh | 858 | 0.004–0.04 | 0.301 | 0.280 | 0.005 | 0.94 |
| | After 12 cycles - MWSA | 870 | 0.004–0.04 | 0.280 | 0.270 | 0.007 | 0.96 |
| | After 12 cycles -TSA | 863 | 0.004–0.04 | 0.260 | 0.270 | 0.006 | 0.97 |
| | | | | | | | |
| 13X | Fresh | 690 | 0.003–0.02 | 0.347 | 0.220 | 0.092 | 0.45 |
| | After 12 cycles - MWSA | 689 | 0.003–0.02 | 0.325 | 0.218 | 0.093 | 0.46 |
| | After 12 cycles -TSA | 684 | 0.003–0.02 | 0.334 | 0.215 | 0.090 | 0.47 |

$V_{mes\,o}$ (cm³/g): mesopore volume (Hybrid DFT); $W_0$ (cm³/g): total micropore volume at p/p0 < 0.1; $D$ (nm): average micropore width.

The impact of the thermal treatment and consecutive cyclic operations (heating and cooling) on the surface area and pore structure of the spent adsorbents were measured and compared with the fresh samples (Fig. 8 and Table 2). Modification to the textural properties (i.e. an increase in surface area and total pore volume) of porous adsorbents by microwave regeneration has been previously reported [30], however, results in this study show how the $N_2$ adsorption isotherms of regenerated samples almost overlap with those of fresh samples, and that no changes in the surface area or pore sizes and pore volumes are observed. In theory, in order to see an appreciable increase or decrease in pore volume and/or pore size, a degree of activation or structural annealing should take place, which clearly did not occur for the adsorbents tested in this study under the operating conditions used in the gas separation processes. Therefore, neither of the regeneration methods used in this study altered the structural integrity of the adsorbents, which indicates the stability of the selected adsorbents for this application. From Table 2 and Fig. 9 it can be concluded that the surface area and pore volumes were not affected by the swing adsorption cycles.

**Fig. 9**
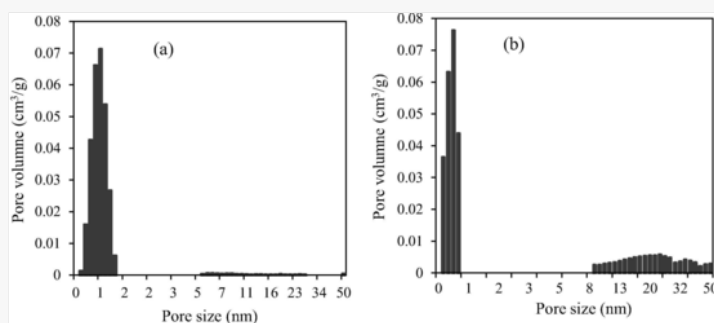


(b) Pore size distribution of fresh samples of (a) Norit R and (b) 13X.

Fig. 8b and c show the pore size distribution of Norit R and 13X evaluated using the DFT method. It is apparent that the micropore size distribution of Norit R displays a spread over the whole micropore range (0–2 nm), consistent with the average micropore size ($D$ = 0.94 nm) in Table 2, evaluated from Dubinin- Stoeckli empirical expression for average micropore width ($L_0$) [31]. A broad pore size range of mesopores (6–30 nm) is also present in the structure, although their pore volume is insignificant compared to micropore volume (0.005 cm³/g). 13X exhibits a much narrower micropore size distribution (0.25–0.60 nm) which is again in line with the average micropore size ($D$ = 0.45 nm) in Table 2.

This could, in part, explain the high $CO_2$ capacity of 13X as its average micropore size is closer to the kinematic diameter of $CO_2$ (0.33 nm) [32] than Norit R. As deduced from the shape of the isotherm and the existence of a hysteresis loop, the pore size distribution curve of 13X reveals the presence of mesopores of size ranging from 9 to 50 nm.

## 4 Conclusions

Two commercially available adsorbents, an activated carbon (Norit R2030$CO_2$) and a zeolite (13X), were used to compare the performance of microwave-assisted regeneration with conventional regeneration in swing adsorption cycles for a simulated pre-cleaned and dry flue gas representative to post-combustion. The results demonstrate that microwave heating could be a feasible alternative to conventional heating in the cyclic swing adsorption process for post-combustion capture if the selection of the sorbent material and the operating conditions are the adequate. This study shows a preliminary investigation on commercial sorbents with certain operating conditions, however further room to investigate the real feasibility of the process in different operating scenarios are needed to find out whether MWSA could led to an improved $CO_2$ capture technology with less energy consumption compared with conventional thermal swing. Overall, the data present a mixed outcome where MWSA shows a slight advantage over the TSA in some respects and vice versa. With the activated carbon, the cyclic capture capacity and the regeneration efficiency are stable in both heating modes but marginally better with MWSA, whereas for the zeolite, the regeneration technologies appear to be indifferent and poorer in some instances with microwave heating, such as the power uptake, under the regenerating conditions tested.

Similar $CO_2$ desorption rate is observed in both TSA and MWSA for both adsorbents with almost overlapping desorption profiles in the early stage of the regeneration, however, a difference is observed for the decreasing desorption rate in the last part of the regeneration profiles which indicate faster $CO_2$ desorption rates with microwave heating. Additionally, the activated carbon shows a marginally higher maximum desorption rate with MWSA than with TSA, whereas for the zeolite, the maximum rate is lower with MWSA compared to TSA.

Regarding power consumption, microwave regeneration led to energy savings over conventional regeneration with the activated carbon. Power uptake per sample unit mass and per amount of $CO_2$ removed are lower by 18.69 and 17.76% respectively in MWSA compared with TSA. With 13X, however, power uptake is greater in MWSA than in TSA. This is rooted in the difference between the instrument sizes of the two heating sources, and the nature of the interaction of the adsorbent with microwave irradiation. The heating time required to regenerate 80, 90 and 100% was found to be shorter with TSA in both adsorbents. With Norit R, it took 4.0, 4.5 and 7.8 mins more with MWSA compared to TSA to achieve the previously indicated regeneration percentages, in the same order. Similar results were also observed with 13X, but in this case the time difference between TSA and MWSA was slightly greater (i. e. 4.2, 6.5 and 27 mins more with MWSA to obtain similar regeneration percentages in the order mentioned above).

Finally, post-cyclic analysis on the adsorbents reveals no effect on the textural properties, indicating material stability after 12 adsorption regeneration cycles.

## 5 Future recommendations

The activated carbon heated much faster than 13X with MWSA compared to TSA, yet to achieve the same extent of regeneration, more time was needed in MWSA cycles. The origin of this should be further investigated to determine the main reasons for this difference. For example, using exactly equal heating power in both processes. These tests can also be repeated with different feed gas compositions in the presence of moisture and observe the effect on the extent of regeneration with time.

The regeneration power used here was deemed to be below the threshold for 13X, therefore higher power which could induce quicker thermal response should be investigated. Regeneration temperatures above 100 °C should also be considered for 13X. The feed gas used in this case was a binary gas consisting of $CO_2$ and $N_2$ (15/85% v/v). Different percentages of water vapour in the flue gas can be further tested to assess its impact on thermal response, working capacity, $CO_2$ uptake and regeneration. Also, an increase in the number of cycles from 12 to as many as possible and observe under which regeneration method the material integrity of the adsorbents is preserved the longest may be worth studying.

Finally, after a further investigation on the process operating parameters, such as the indicated above, an estimation of the volumetric $CO_2$ working capacity and energy consumption could be scaled up to stablish essential comparison with more mature CCS technologies.

## CRediT authorship contribution statement

**M.M. Yassin:** Investigation, Data curation, Writing – original draft, Writing – review & editing. **J.A. Anderson:** Writing – review & editing. [Instruction: text in references (Supplementary) to be justified][Instruction: Can't seem to be

able to change format (i.e. bold font etc).)]G.A.Dimitrakis: resources (dielectric properties). **C.F. Martín:** Conceptualization, Methodology, Writing – review & editing, Visualization, Supervision, Funding acquisition.

## Declaration of Competing Interest

## Acknowledgment

## Appendix A Supplementary material

Table S1. Point of Zero charge, elemental analysis, and chemical analysis. Supplementary data to this article can be found online at https://doi.org/10.1016/j.seppur.2021.119326.

## References

> ⓘ The corrections made in this section will be reviewed and approved by a journal production editor. The newly added/removed references and its citations will be reordered and rearranged by the production team.

[1] Abu-Zahra M.R.M., Abbas Z., Singh P., Feron P., Carbon dioxide post-combustion capture: solvent technologies overview, status and future directions, Mater. Process. Energy Commun. Curr. Res. Technol. Dev. (2013) 923–934.

[2] Zhang W., Sun C., Snape C.E., Irons R., Stebbing S., Alderson T., et al., Process simulations of post-combustion CO$_2$ capture for coal and natural gas-fired power plants using a polyethyleneimine/silica adsorbent, Int. J. Greenh. Gas Control 58 (2017) 276–289, doi:10.1016/j.ijggc.2016.12.003.

[3] Martín C.F., Sweatman M.B., Brandani S., Fan X., Wet impregnation of a commercial low cost silica using DETA for a fast post-combustion CO$_2$ capture process, Appl. Energy 183 (2016) 1705–1721, doi:10.1016/j.apenergy.2016.09.081.

[4] Martín C.F., García S., Beneroso D., Pis J.J., Rubiera F., Pevida C., Precombustion CO$_2$ capture by means of phenol-formaldehyde resin-derived carbons: from equilibrium to dynamic conditions, Sep. Purif. Technol. 98 (2012) 531–538, doi:10.1016/j.seppur.2012.03.017.

[5] S. Kwon, M. Fan, H.F.M. DaCosta, A.G. Russell, K.A. Berchtold, M.K. Dubey, CO2 Sorption, Elsevier Inc., 2010. https://doi.org/10.1016/b978-0-8155-2049-8.10010-5.

[6] Bonnissel M.P., Luo L., Tondeur D., Rapid thermal swing adsorption, Ind. Eng. Chem. Res. 40 (2001) 2322–2334, doi:10.1021/ie000809k.

[7] Cherbański R., Molga E., Intensification of desorption processes by use of microwaves – an overview of possible applications and industrial perspectives, Chem. Eng. Process. Process Intensif. 48 (2009) 2, doi:10.1016/j.cep.2008.01.004.

[8] Cherbański R., Komorowska-Durka M., Stefanidis G.D., Stankiewicz A.I., Microwave swing regeneration Vs temperature swing regeneration – comparison of desorption kinetics, Ind. Eng. Chem. Res. 50 (2011), doi:10.1021/ie102490v.

[9] P. Di, D.P.Y. Chang, Microwave regeneration of volatile organic compound (VOC) adsorbents, University of California, Davis, n.d., pp. 1–12.

[10] Fayaz M., Shariaty P., Atkinson J.D., Hashisho Z., Phillips J.H., Anderson J.E., et al., Using microwave heating to improve the desorption efficiency of high molecular weight VOC from beaded activated carbon, Environ. Sci. Technol. 49 (2015) 4536–4542, doi:10.1021/es505953c.

[11] Cherbański R., Regeneration of granular activated carbon loaded with toluene – comparison of microwave and conductive heating at the same active powers, Chem. Eng. Process. Process Intensif. 123

Q10

(2018) 148–157, doi:10.1016/j.cep.2017.11.008.

[12] McGurk S.J., Martín C.F., Brandani S., Sweatman M.B., Fan X., Microwave swing regeneration of aqueous monoethanolamine for post-combustion $CO_2$ capture, Appl. Energy 192 (2017) 126–133, doi:10.1016/j.apenergy.2017.02.012.

[13] Çalişkan E., Bermúdez J.M., Parra J.B., Menéndez J.A., Mahramanlioĝlu M., Ania C.O., Low temperature regeneration of activated carbons using microwaves: revising conventional wisdom, J. Environ. Manage. 102 (2012) 134–140, doi:10.1016/j.jenvman.2012.02.016.

[14] Zhang L., Jiang H., Ma C., Yong D., Microwave regeneration characteristics of activated carbon for flue gas desulfurization, J. Fuel Chem. Technol. 40 (2013) 1366–1371, doi:10.1016/s1872-5813(13)60004-3.

[15] Yagmur E., Turkoglu S., Banford A., Aktas Z., The relative performance of microwave regenerated activated carbons on the removal of phenolic pollutants, J. Clean. Prod. 149 (2017) 1109–1117, doi:10.1016/j.jclepro.2017.02.188.

[16] Webley P.A., Zhang J., Microwave assisted vacuum regeneration for $CO_2$ capture from wet flue gas, Adsorption 20 (2014) 201–210, doi:10.1007/s10450-013-9563-y.

[17] Chronopoulos T., Fernandez-Diez Y., Maroto-Valer M.M., Ocone R., Reay D.A., Utilisation of microwave energy for $CO_2$ desorption in postcombustion carbon capture using solid sorbents, Energy Proc. 63 (2014) 2109–2115, doi:10.1016/j.egypro.2014.11.227.

[18] Nígar H., García-Baños B., Peñaranda-Foix F.L., Catalá-Civera J.M., Mallada R., Santamaría J., Amine-functionalized mesoporous silica: a material capable of $CO_2$ adsorption and fast regeneration by microwave heating, AIChE J. 62 (2016) 547–555, doi:10.1002/aic.

[19] Yang J., Tan H.Y., Low Q.X., Binks B.P., Chin J.M., $CO_2$ capture by dry alkanolamines and an efficient microwave regeneration process, J. Mater. Chem. A 3 (2015) 6440–6446, doi:10.1039/c4ta06273f.

[20] A. Dyer, Encyclopedia of materials: science and technology, second ed., Zeolites (2006) 1–5.

[21] Sing K.S.W., Everett D., Haul R., Moscou L., Pierotti R., Rouquerol J., et al., Reporting physisorption data for gas/solid systems with special reference to the Determination of Surface Area and Porosity (Recommendations 1984)Reporting physisorption data for gas/solid systems with special reference to the determination of surface area and porosity (Recommendations 1984), International Union Pure Appl. Chem., Phys. Chem. Div., Comm. Colloid Surf. Chem. Incl. Catal. 57 (1985) 603–619.

[22] Pevida C., Plaza M.G., Arias B., Fermoso J., Rubiera F., Pis J.J., Surface modification of activated carbons for $CO_2$ capture, Appl. Surf. Sci. 254 (2008) 7165–7172, doi:10.1016/j.apsusc.2008.05.239.

[23] Noh J.S., Schwarz J.A., Estimation of the point of zero charge of simple oxides by mass titration, J. Colloid Interface Sci. 130 (1989) 157–164, doi:10.1016/0021-9797(89)90086-6.

[24] Parra B., Ania C.O., Figini-albisetti A., Velasco L.F., Applied surface science effect of outgassing temperature on the performance of porous materials, Appl. Surf. Sci. 256 (2010) 5182–5186, doi:10.1016/j.apsusc.2009.12.090.

[25] Turner M.D., Laurence R.L., Conner W.C., Yngvesson K.S., Microwave radiation's influence on sorption and competitive sorption in zeolites, AIChE J. 46 (2000) 758–768, doi:10.1002/aic.690460410.

[26] J.G. MacDowell, Microwave heating of nepheline glass-ceramics, vol. 63, 1984. https://doi.org/10.1021/nl904053j.

[27] Whittington B.I., Milestone N.B., The mcirowave heating of zeolites, Zeolites 12 (1992) 815–818, doi:10.1016/0144-2449(92)90055-T.

[28] Guo Y., Zhang H., Liu Y., Desorption characteristics and kinetic parameters determination of molecular sieve by thermogravimetric analysis/differential thermogravimetric analysis technique, Adsorpt. Sci. Technol. 36 (2018) 1389–1404, doi:10.1177/0263617418772665.

[29] Gallei E., Stumpf G., Infrared spectroscopic studies of the adsorption of carbon dioxide and the coadsorption of carbon dioxide and water on CaY- and NiY-zeolites, J. Colloid Interface Sci. 55 (1976) 415–420, doi:10.1016/0021-9797(76)90051-5.

[30] Ania C.O., Parra J.B., Menéndez J.A., Pis J.J., Microwave-assisted regeneration of activated carbons loaded with pharmaceuticals, Water Res. 41 (2007) 3299–3306, doi:10.1016/j.watres.2007.05.006.

[31] Stoeckli F., López-Ramón M.V., Hugi-Cleary D., Guillot A., Micropore sizes in activated carbons determined from the Dubinin-Radushkevich equation, Carbon N Y 39 (2001) 1115–1116, doi:10.1016/S0008-6223(01)00054-9.

[32] Nabavi S.A., Vladisavljević G.T., Zhu Y., Manović V., Synthesis of size-tunable $CO_2$-philic imprinted polymeric particles (MIPs) for low-pressure $CO_2$ capture using oil-in-oil suspension polymerization, Environ. Sci. Technol. 51 (2017) 11476–11483, doi:10.1021/acs.est.7b03259.

## Highlights

- Steadier cyclic $CO_2$ uptake with microwave-assisted regeneration ~~than with conventional regeneration~~ for Norit R ~~the activated carbon (Norit R2030CO₂)~~.
- Higher maximum desorption rate with microwave-assisted regeneration for ~~the activated carbon~~ (Norit R~~2030CO₂) and smaller for zeolite 13X~~.
- ~~More stable regeneration efficiency with microwave heating for the activated carbon (Norit R2030CO2).~~ More stable regeneration efficiency with microwave heating for Norit R.
- ~~Higher regeneration rate with microwave-assisted regeneration in later stages of the desorption for the adsorbents tested.~~ Higher regeneration rate with microwave in later stages of the desorption.
- ~~Preservation of adsorbents' textural integrity in the cyclic microwave swing adsorption (MWSA).~~ · Adsorbents' textural properties prevail with cyclic microwave swing adsorption.

# Appendix A Supplementary material

The following are the Supplementary data to this article:

Multimedia Component 1

**Supplementary data 1**

## Queries and Answers

**Q1**

**Query:** Please check the edit(s) made in article title, and correct if necessary.

**Answer:** correct

**Q2**

**Query:** Your article is registered as a regular item and is being processed for inclusion in a regular issue of the journal. If this is NOT correct and your article belongs to a Special Issue/Collection please contact a.chinnappan@elsevier.com immediately prior to returning your corrections.

**Answer:** Yes

**Q3**

**Query:** The author names have been tagged as given names and surnames (surnames are highlighted in teal color). Please confirm if they have been identified correctly.

**Answer:** Yes